Manufacturing and Characterization of Novel Multilayer Magnets for Electrical Machine Applications

Manufacturing and Characterization of Novel Multilayer Magnets for Electrical Machine Applications

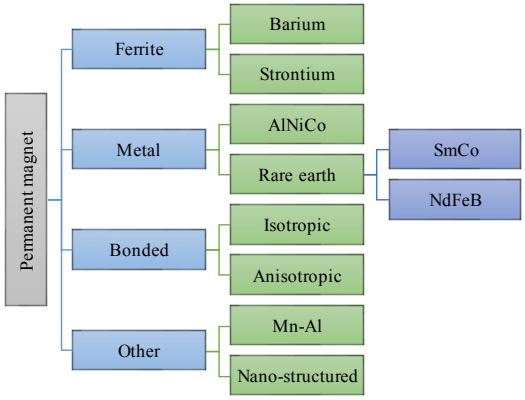

Fig. 1. Permanent magnet types.

This newly developed hybrid magnetic material has been considered for sensor application; however, it could also be exploited in electrical machine applications under a circumstance described later on.

In [11], the authors have proposed the concept of multiple layer compression of soft magnetic composite together with bonded magnet material to realize a unified magnetic block. In particular, three conditions have been investigated, (i) three layers samples consisting of one layer made of hard magnetic material sandwiched between two layers made of soft magnetic material, (ii) double-layer compaction of hard and soft materials, and (iii) double-layer compaction of two different hard materials. The compaction of triple-layer samples was failed, but the double-layer samples were satisfactory. However, the different young's modulus of elasticity of the soft and hard parts caused no appreciable convexity issues in the surfaces of the produced samples. Recently, a new category of permanent magnet electrical machines has been introduced, so-called variable-flux permanent magnet synchronous machines (VF-PMSMs), also known as "*memory machines*". They can improve the loss reduction capability in the flux weakening region by manipulating the magnetization state. In more detail, the flux linkage produced by the magnets can be controlled by injecting large current pulses through the stator windings to partially demagnetize the magnets [12]–[17].

It was already shown that the adoption of two magnets, one with high coercive force and the other one with low coercive force, could improve the machine's flux weakening capability. In variable flux PM synchronous machines, the '*weak*' and '*strong'* magnets can be positioned in series (Fig. 2a) or parallel (Fig. 2b) configuration.

In [18], the authors have experimentally investigated the compaction of several double-layer hard magnetic materials having different magnetic and mechanical properties in order to acquire a unified multilayer layer magnet block for electrical machine applications, and the built samples have been initially characterized.

The performance of an external rotor surface-mounted permanent magnet synchronous motor equipped with multilayer magnets has been evaluated through FEM simulations in [19]. It was observed that applying this technology can improve machine performance and reduce the cost of materials as well.

Fig. 2. Variable flux PM synchronous machine configurations (red: low coercive force magnet, green: high coercive force magnet): a) series magnet; b) parallel magnet. (adopted from [16])

In this paper, the authors further develop previous research on producing and characterizing innovative multilayer structures of powdered magnetic materials. More specifically, the study focuses on the interesting case of multilayer magnets produced compacting materials having different magnetic and mechanical properties. The reported analyses aim to assess their applicability for building special PM machines, like the above-mentioned VF-PMSMs.

II. Self-Produced Permanent Magnets

In this study, two different self-produced compositions of hard materials have been considered to build the multilayer samples. In detail, NdFeB-based bonded and hybrid materials have been utilized to produce the samples. The two are categorized as hard materials.

A. Bonded Magnet

Bonded magnets consist of high coercivity powder and thermoset polymers for compaction molding, thermoplastic polymers for injection/extrusion molding, and elastomer polymers for extrusion/calendaring. Depending on the production process, the powder can be hard ferrite, NdFeB, and in particular cases also SmCo and AlNiCo. Generally, minimum possible additives are mixed in the compaction molding process. Therefore, the obtained magnet has a higher remanent flux density and BH_{max} as in other production technologies. Moreover, loading factor and molding parameters are crucial in obtaining a magnet with appropriate magnetic and mechanical properties. For this study, a specific NdFeB powder for bonded magnets (the MQP-14-12 for high-temperature applications) and a phenolic resin were used to prepare the samples. Fig. 3 shows the demagnetization curves of the phenolic bonded magnet in the lab. The innovative compaction process guarantees exceptional compaction of 99% of NdFeB magnetic powder and only 1% phenolic resin.

B. Hybrid Magnet

Hybrid magnets can be built similarly to the bonded magnets by means of compaction molding. In order to prepare the required materials, the same powder utilized for the bonded magnet has been mixed with a soft magnetic powder (e.g. very pure iron powder), thus resulting in a lower hard magnetic material percentage.

A very small percentage of phenolic resin is still added to acquire a satisfactory mechanical resistance [8]. A large number of samples having different grades of hybrid magnetic powder have been prepared and characterized in the lab allowing the fine-tuning of the process and the tailoring of the material characteristics [8].

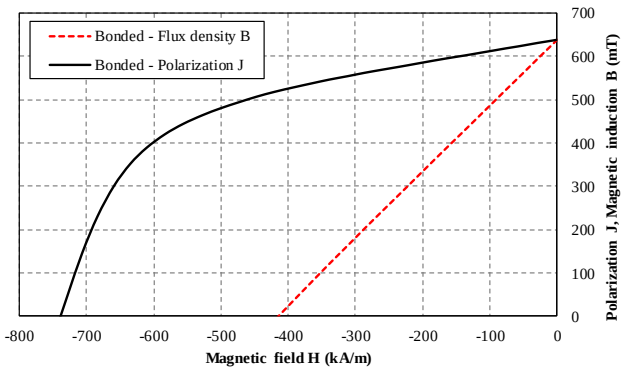

Fig. 3. Demagnetization curve of the bonded magnet using phenolic resin.

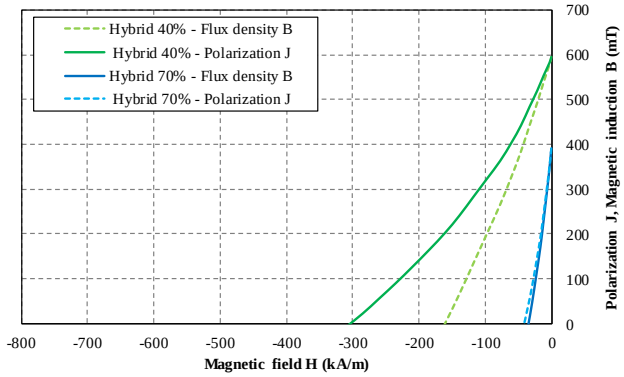

Fig. 4. Demagnetization curves of the hybrid 40 % and hybrid 70 %.

TABLE I
THE MAIN PROPERTIES OF THE SELF-PRODUCED SINGLE-LAYER MAGNETS AT 20°C.

Type of magnet	Bonded	HMC-40	HMC-70
B_r, (T)	0.639	0.596	0.390
H_{cJ}, (kA/m)	738.6	303.3	41.4
H_{cB}, (kA/m)	414.7	160.8	34.8
BH_{max}, (kJ/m^3)	67.2	20.6	2.85

It is worth remembering that the grade of powder materials is correlated to the weight of the pure iron powder and resin. For this study, two grades of hybrid magnets consisting of 40% and 70% iron content in the weight have been produced.

Fig. 4 shows the demagnetization curve of the hybrid magnet samples, while Table I represents the main characteristic of the self-produced bonded and hybrid magnets. In detail, it should be noted that the values of the energy product BH_{max}, remanence B_r, and coercive force H_c of the materials can be tailored according to the application needs. In particular, the use of HMC materials makes the magnets not only weaker but also easier to magnetize or demagnetize in situ. This is due to increased magnetic permeability and reduced coercivity. As a result, they are particularly suitable for use in multilayer structures, as explained in the next chapter.

III. MULTILAYER PERMANENT MAGNET

The proposed pressing technology allows to completely remove the parasitic air gaps among discrete PM blocks due to the thickness of glue used in the conventional assembling process of electrical machines. In fact, this attractive solution improves the magnetic and mechanical properties of the block.

The feasibility of multilayer compaction of hard and soft magnetic materials has been proved in [11]. Here the focus is on simultaneous compression molding of different types of hard magnetic materials. However, due to the hydraulic press available in the lab and the selected application, only the double-layer PM solution has been investigated in this study. Hence, using the magnetic materials listed in Table 1, it was possible to produce the double-layer samples. Fig. 5 shows the two samples of double-layer magnet built in the lab: the sample at the right consists of one layer of bonded magnets and one layer of hybrid 40 %, while the sample on the left uses the same bonded magnet but the second layer of hybrid 70 %.

To build the double-layer samples, a defined volume of the mold has been initially filled by bonded material. Then, a small pressure (around 100MPa) was applied to slightly compact the materials in the mold. After that, a specific volume of the mold was filled again by hybrid material. Finally, a high pressure, around 600 MPa, was applied. It should be remarked that the thickness of each layer can be computed in advance based on the compaction coefficient of selected materials. So, it is possible to produce multilayer magnets having different thicknesses for each layer. In this study, the thickness of each layer has been considered equal.

It should also be pointed out that the mechanical characteristics of the selected materials were not equal due to their different percentage of pure iron powder. As reported in [11], the compressing molding process of soft and hard magnetic materials with different Young's modules can lead to final geometrical/structural problems, such as unwanted convexity and even cracks due to internal stresses. This is related to the different elastic springback effects between the materials. However, since Young's modulus of elasticity of the hybrid materials is close to that of the bonded materials, no cracks or convexity issues were found on the built samples – see Fig. 5.

Generally speaking, two possible magnetization directions can be accomplished for the double-layer magnet block shown in Fig. 5: (i) along a horizontal axis and (ii) along the vertical axis. Therefore, by selecting the appropriate magnetization direction, the same mold can obtain the parallel and series PM arrangements. Noticeably, the maximum thickness of the layers and all the other overall dimensions of the sample depends on the available hydraulic press size. Therefore, in order to have a comprehensive understanding, both magnetization directions of the double-layer magnets are considered in the research.

Fig. 5. Double-layer samples formed by bonded and hybrid magnets (on the left hybrid 70 % and on the right hybrid 40 %).

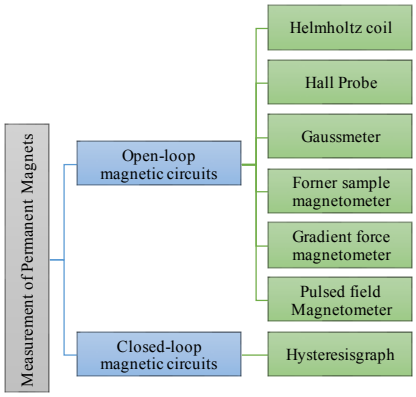

Fig. 6. Measurement methodologies for permeant magnets.

IV. Overview of The Measurement Techniques Of Permanent Magnets

As shown in Fig. 6, two measurement approaches could be employed to characterize permanent magnets: (i) the open magnetic circuit (ii) the closed magnetic circuit. The open magnetic circuit techniques are based on determining the magnetic moment of the magnet, while the closed magnetic circuit techniques are based on fluxmetric methods. The closed magnetic circuit methods provide the absolute *B-H* and *J-H* curves.

However, this approach may not be appropriate for the magnets having very high coercive force due to the natural constraint in iron saturation. On the other side, open magnetic circuit methods require some reference points for calibration that sometimes lead to a small percent of uncertainties [20]. For expediency, a brief summary of the renowned measurement techniques is presented as follows. However, the previously mentioned methods are the most popular measurement methods used for hard magnetic materials. Some other measurement methodologies, such as 3D mapper and quantum methods, are taken into account only for particular applications. Thus, they are not described in this paper.

A quick and traditional method is based on Helmholtz coils. It consists of a pair of identical circular shape coils connected in series and placed symmetrically on the same axis and separated by a distance as long as their radius. The measuring procedure is very easy and low-cost [21]; and a non-destructive way to test the magnets, but only measures a single point on the magnetization curve [22]. Another technology-based on fast method and single-point measurement is Hall probe [23]. The working principle of this technique is based on the hall effect. Furthermore, Hall probe is the easiest and most flexible measurement solution of the magnetic fields generated by magnets, and combined with a gaussmeter can measure magnetic induction of air gaps in electrical motors. The different solution can be represented by a vibrating sample magnetometer (VSM) consisting of an electromagnet, pickup coils, and a load speaker membrane to vibrate the sample. The magnet oscillates perpendicularly to an external uniform magnetic field generated by the electromagnet, and the sensing coils detect the magnetic moment [24]. This measurement instrument is a simple, inexpensive, and versatile method, and it can be employed for both soft and hard magnetic materials. In addition, the size of the sample is restricted (very small samples in a range of a few millimetres) [25]. Gradient force magnetometer is also known as a vibrating reed magnetometer. Such a method is only used for measuring magnetic moment lower than the VSM noise floor, as small as 10-11 emu [20]. Instead, the magnetic materials with very high values of coercive force and energy product can be measured with a pulsed field magnetometer. In this method, a capacitor bank is discharged through a solenoid to generate a large magnetic field. A pickup coil positioned around the sample detects the generated field. This approach is non-destructive and fast and can be employed for arbitrary geometries. However, the presence of eddy current restricts the use of this method only to the ferrite magnets due to their high insulating properties [24], [25].

Hysteresisgraph unquestionably is the most common industrial instrument which allows acquiring the full intrinsic characterization of magnets. In this measurement method, the magnet is placed in a closed magnetic circuit, having two polar pieces that can be adjusted to close the gap. It should be highlighted that the pole surfaces should be flat, parallel, and perpendicular to the direction of magnetization. A sensing coil is positioned around the sample to measure the produced magnetic induction of the magnet. An external field is applied during the test by electromagnets that are part of the closed magnetic circuit. To measure the applied field, a test coil or a hall probe is usually deployed that is placed within the gap and next to the magnet. The main advantage of using a hysteresisgraph is that no demagnetization correction is required [25]–[27]. The available hysteresisgraph-based measurement system is shown in Fig. 7. This system has been used to measure the self-produced bonded magnet and hybrid magnet demagnetization curves, as shown previously in Fig. 3 and Fig. 4, respectively.

V. Experimental Test Results

The magnetic characteristics of the produced samples can be directly obtained by testing the final device prototypes, which may not be rational due to the very high expenditure, or simply using a closed magnetic circuit parameter by applying recognized technique such as the procedure specified in the IEC 60404-5 [28].

Two tests have been carried out on each sample using the available hysteresisgraph to characterize the series and parallel arrangement of the double-layer magnets. The first test is a conventional test in accordance with the measurement of magnetic properties described in [28]. For the second testing approach, a specific magnetic circuit with a very small air gap length has been designed due to the analogy with the magnetic circuit of a rotating electrical machine, in which the air gap is always present for obvious functional reasons. Therefore, a '*dummy*' pole piece made of soft material has been taken into consideration to define an adjusted air gap along the magnetic circuit, as shown in Fig. 8.

It should be remarked that the available hysteresisgraph can inject large current values that are required to fully demagnetize the samples, even with an air gap along its magnetic circuit. The induction in the air gap has been measured by means of a gaussmeter, while the magnetization and magnetic field in the sample has been measured with the hysteresisgraph coils connected to the instrument's fluxmeter.

Fig. 7. The hystersisgraph: view of the measurement system.

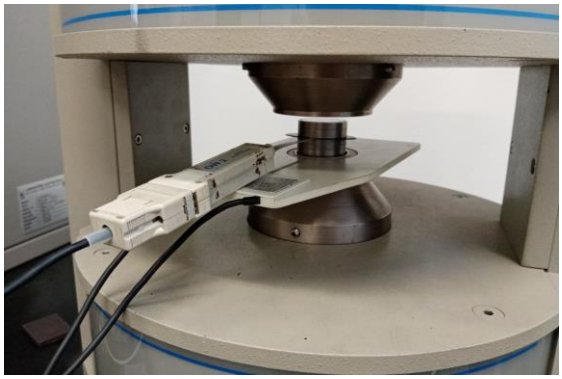

Fig. 8. Measurement of air gap flux density by means of the introduction of gaussmeter in the hysteresisgraph

As shown in Fig. 9, an additional soft iron cylinder has been used to direct the flux lines exiting from the magnet toward the magnetic circuit. The correct sample characterization was in this way achieved together with the newly introduced air gap induction. The hysteresisgraph contains two series-connected coils that were employed in characterizing the magnets. It should be remarked that the multilayer magnets had been magnetized when the test procedure began. In order to emulate the demagnetization effect in a variable flux machine (see [15]), a DC has been injected into the coils in order to create a magnetic field in the opposite direction of the field generated by the permanent magnets. Then, the current amplitude has progressively increased until the magnet placed in the hysteresisgraph was completely demagnetized. The magnetic induction (B) and polarization (J) in the magnet arrangement and air gap flux density have been recorded for each current value. The flux density in the air gap has been measured employing a gaussmeter, as shown in Fig. 8.

Being the DC current regulation automatic, the synchronization of all measurement devices plays a key role in obtaining matching values. Finally, concerning Fig. 9, the magnetization direction of the 'strong' magnets (bonded magnets) and the 'weak' magnets (the hybrid 40% or hybrid 70 %) is vertical (i.e., parallel to the Y-axis), both for the parallel and series arrangements.

A. Series configurations

The double-layer magnets shown in Fig. 9 have been tested on the basis of the previously explained procedures, standard closed magnetic circuit with and without an airgap along the magnetic, in order to obtain the demagnetization curve of the magnet in the second quadrant. Fig. 10 shows the polarization and the flux densities generated by the double-layer magnets with a series arrangement using the standard closed magnetic circuit without an air gap. In detail, 'series 40 %' consists of the layer of the hybrid magnet 40 %, and 'series 70 %' has the layer of the hybrid magnet 70 %. As expected, the double-layer sample containing hybrid material with more iron content (hybrid magnet 70 %) is weaker than the one with more bonded materials (hybrid magnet 40 %). Consequently, the tests carried out on the series arrangements reveal that the double-layer samples enjoying less pure iron powder (hybrid magnet 40 %) require more magnetic fields to be demagnetized. In more detail, the single-layer bonded magnet sample needs 410 kA/m to be completely demagnetized the magnet in the same magnetic circuit, while the series 40 % and series 70% samples are around 580kA/m and 371 kA/m, respectively.

It can be concluded that if double-layer magnets are used, a lower level of field and consequently current are required to decrease the working point of the magnet. The demagnetization current 'saving' is greater with double-layer magnets utilizing a softer hybrid part, leading to potential energetic improvements during flux weakening operation in variable flux PM machines.

The samples have been tested using a closed magnetic circuit with a small air gap to deeply investigate and prove this concept, as shown in Fig. 8. The flux density in the air gap has been measured using a gaussmeter. Fig. 11 shows the flux densities in the air gap vs. current values. The bonded 'plus' hybrid magnet 70 % requests less current to acquire the same air gap flux density with respect to the bonded plus hybrid magnet 40 % counterpart. However, the air gap flux is nearly similar when the current in the coils is equal to zero.

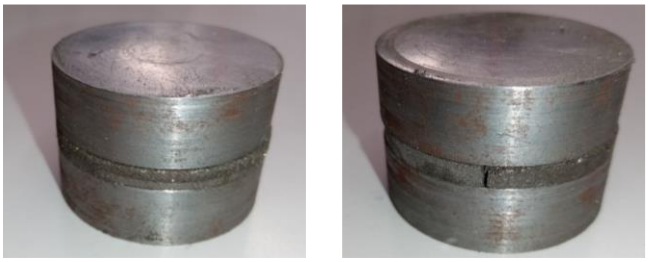

(a) (b)

Fig. 9. Additional soft iron for produced samples, (a): series arrangement, (b): parallel arrangement.

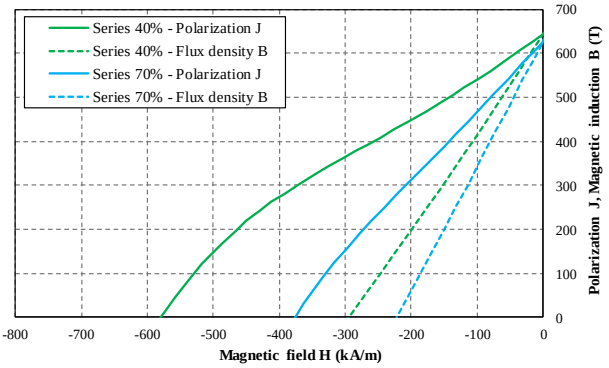

Fig. 10. Measured demagnetization curves for the double-layer magnets with series arrangement.

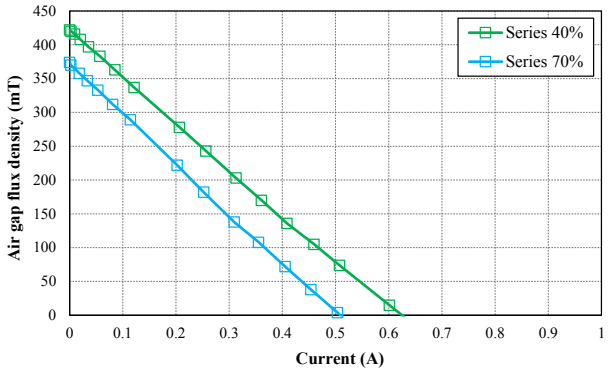

Fig. 11. Measured induction in the air gap vs. current for double-layer samples and series arrangement.

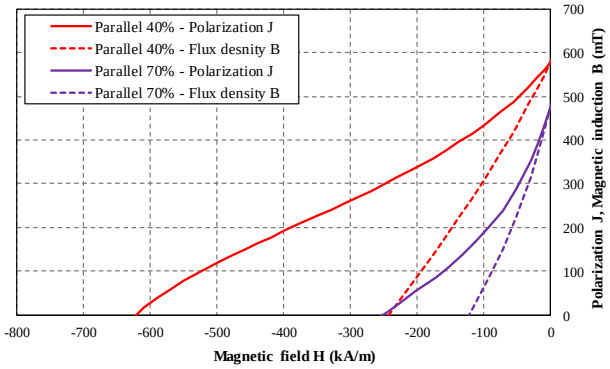

Fig. 12. Measured demagnetization curves for the double-layer magnets with parallel arrangement.

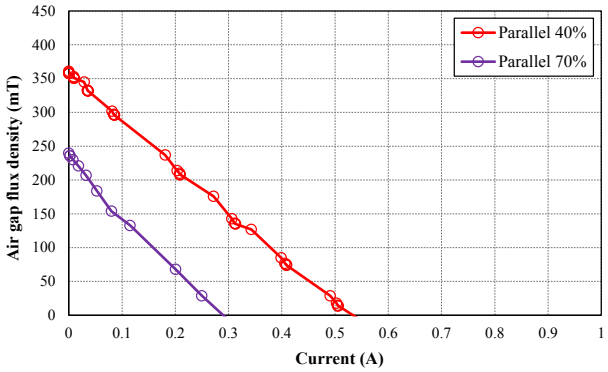

Fig. 13. Measured induction in the air gap vs. current for double-layer samples and parallel arrangement.

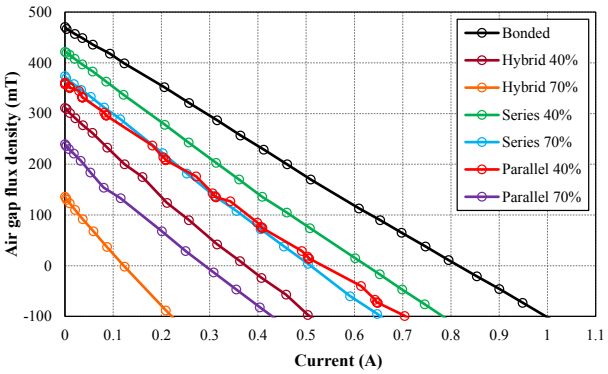

Fig. 14. Comparison of measured induction in the air gap vs. current for all double-layer samples and bonded magnet.

B. *Parallel configurations*

The parallel arrangement samples have been built, magnetized as described at the end of Section III, and placed in the hysteresisgraph to carry out the same tests campaign as for the series arrangements. Thus, Fig. 12 shows the measured demagnetization curves of the double-layer magnets with the parallel arrangement in which the hybrid layer contains 40 % and 70 % iron content ('parallel 40 %' and 'parallel 70 %'), respectively. For the parallel arrangement samples, the tests confirm that the sample containing hybrid materials with less iron content is stronger (both in terms of polarization and coercive force) than the one having fewer hard magnetic materials. However, the variations moving from 40 % to 70 % iron percentage are more evident with respect to the series configuration.

Concerning the demagnetization curve of the bonded magnet, the double-layer samples with parallel configuration need around 615 kA / m (hybrid layer with 40 % iron content) and 250 kA / m (hybrid layer with 70 % iron content) to be completely neutralized. Once again, Fig. 13 presents the measured flux density in the air gap vs. current values for the double-layer samples with the parallel arrangement.

It can be observed that when no current flows into the coils, the measured values of flux density in the air gap is approximately 50 % higher in the sample having more hard magnetic material (parallel 40 %) in comparison with the weaker counterpart. However, reducing the air gap flux density at desired values requires much less current for the parallel 70 % with respect to parallel 40 %.

C. *Remarks*

Comparing the considered arrangements, the double-layer magnet block with the series structure of the strong and weak magnets are stronger than the parallel counterpart. In detail, the remanence flux density and the maximum stored energy in the magnet BH_{max} are higher in the series arrangements with respect to the demagnetization slops of the double-layer magnets, as can be seen in Fig. 10 and Fig. 12.

Also, it is interesting to observe that the parallel 40 % has the maximum value of the coercive force among the multilayer samples while its remanence flux density and its BHmax are lower than both double-layer magnets with the series arrangement. Finally, it should be highlighted that the amount of soft magnetic material used in the hybrid layer affects the produced magnetic field intensity. In other words, the choice of the low coercive magnet is essential to design a double-layer magnet and achieve the desired value of demagnetization field/current. It seems reasonable to conclude that the influence of the bonded magnet layer on the magnetization variation range is much more substantial in the series configuration compared to the parallel configuration. Due to its more comprehensive range of flux regulation capability, the parallel configuration could have a greater Joule loss reduction capability to obtain variable flux operations in the final application. Therefore, both the proposed double-layer magnet arrangements could support a flux weakening operation necessary to obtain high power at high-speed conditions. Fig. 14 has been proposed for a comprehensive overview between all considered double-layers and based materials, bonded and

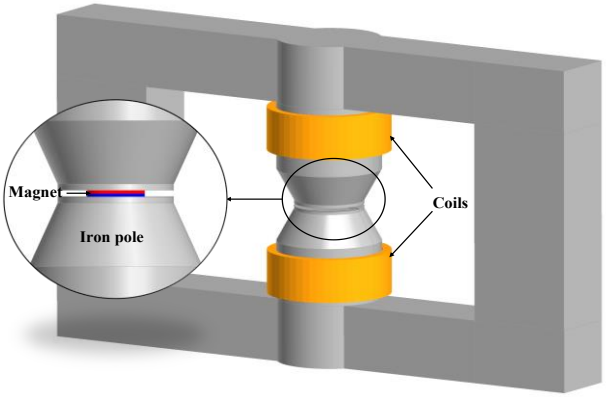

Fig. 15. 3D-FEM model of test setup for the standard test.

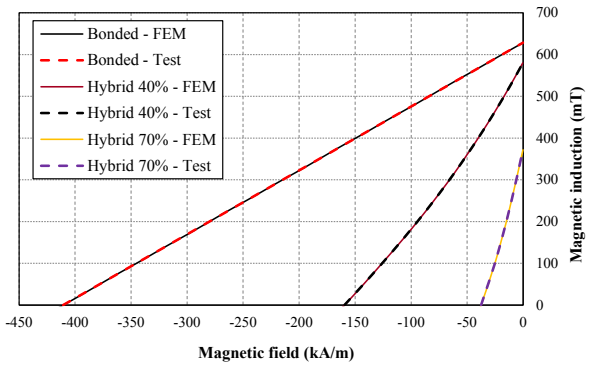

Fig. 16. Comparison of FEM and experimental demagnetization curves of single layer bonded and hybrid magnets.

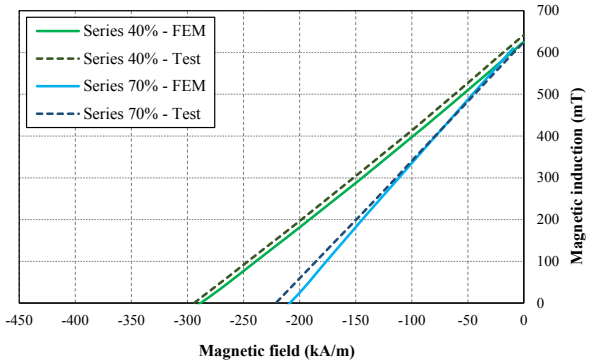

Fig. 17. Comparison of FEM and experimental demagnetization curves of double-layer magnets with series arrangement.

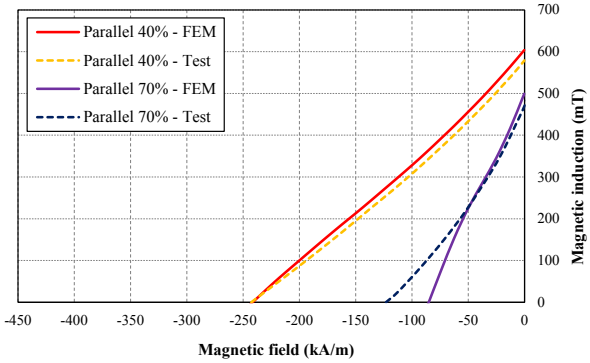

Fig. 18. Comparison of FEM and experimental demagnetization curves of double-layer magnets with the parallel arrangement.

hybrid magnets (Fig. 3 and Fig. 4). The air gap is the same in all the tests. In addition, it is possible to note the difference with the use of multiple layer materials compared to a traditional concept based on bonded magnets.

Finally, it is important to underline that in the magnetic core used for the tests (see Fig. 10), the coils produce a 'direct' demagnetization of the magnets, as happens. For example, a negative d- axis current is supplied for flux weakening in a surface-mounted PM synchronous motor. As in the literature, the variable-flux concept is exclusively reported for internal mounted PM rotor structures. It is expected that the proposed technology could be even more beneficial to exploit the variable-flux capability because the multilayer magnet (that consist of two layers of high and low coercive force hard materials having either series or parallel arrangement) can provide a variable field block of magnet which is applicable in this topology of electrical machines.

VI. FEM Modelling And Experimental Validation

In order to establish a valid simulation approach for future studies, the three-dimensional model of the closed magnetic circuit test setup with and without the defined air gap, including hysteresisgraph and its coils, has been implemented in a commercial finite element (FE) package.

First, the samples have been modeled in the standard magnetic circuit as shown in Fig. 15 to assure that the same characteristics can be achieved, and there is no difference for the characterization of the baseline samples. It should remark that linear material with high relative permeability has been considered for the electromagnet, and the number of coil turns has been initially set equal to one. Fig. 16 compares the magnetic induction vs. magnetic field obtained from simulation and the tests for the baseline materials, bonded and hybrid magnets. As expected, the simulation results are precisely equal to the experimental tests. In addition, Fig. 17 and Fig. 18 show the flux density vs. demagnetizing current for the samples with series and parallel arrangements, respectively. As it can be observed, the values obtained by FEM are perfectly matched with the test results. There is mismatch between simulations and measurements for the parallel 70 % sample due to some unavoidable limitations of the available instruments when used to characterize ‘weak’ magnets. However, the matching in the initial part of the characteristics up to -50 kA/m is assumed adequately good to prove the concept also for this type of magnets.

The second magnetic circuit of the test setup including the air gap and the poles along the magnetic circuit has been implemented in 3D-FEM, as shown in Fig. 19. Since material properties and the number of turns per coil of the hysteresisgraph were not available, the model has been calibrated based on the characteristics of the bonded magnet (shown in Fig. 3) as the baseline. In detail, two points have been considered for the calibration: (i). the maximum induction when there was no current flowing in the hysteresisgraph coils, and (ii) the demagnetization point. For the first point, the air gap length was reduced to have the equal value of the baseline bonded magnet, and for the second point, the demagnetization current was fixed, and the number of turns per coil increased up to reach the demagnetization point of the baseline sample.

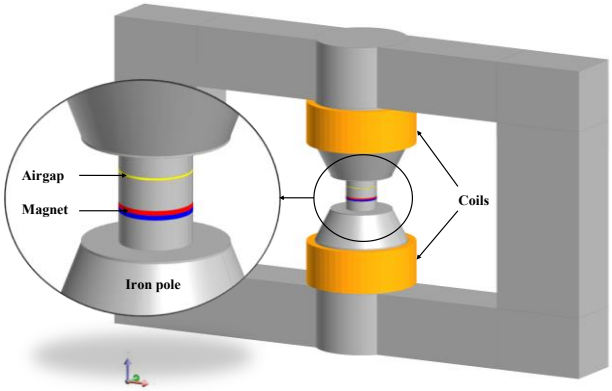

Fig. 19. 3D-FEM model of test setup with the defined air gap.

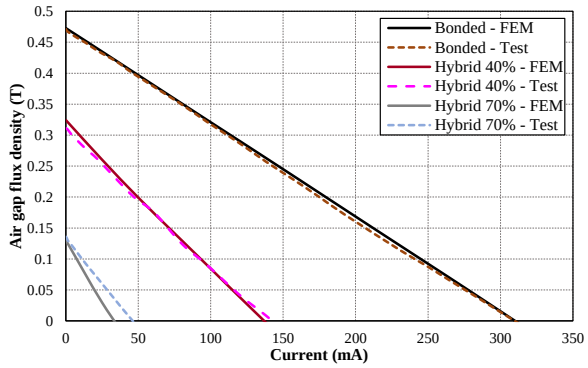

Fig. 20. Comparison of FEM and experimental results of the air gap induction vs. current for single layer.

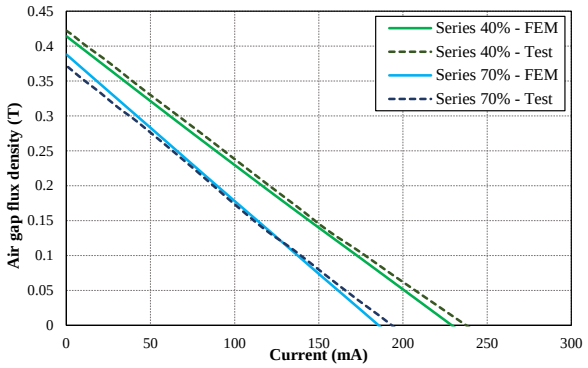

Fig. 21. Comparison of FEM and experimental results of the air gap induction vs. current for double-layer samples with series arrangment.

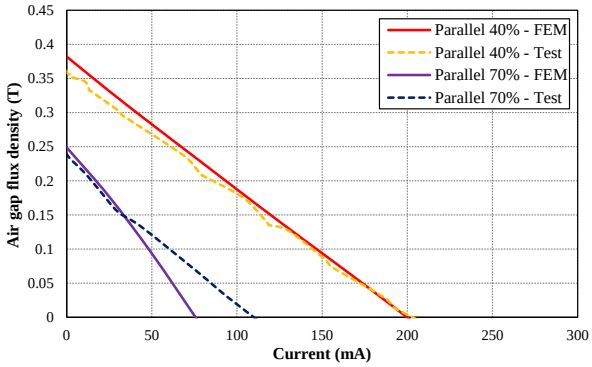

Fig. 22. Comparison of FEM and experimental results of the air gap induction vs. current for double-layer samples with parallel arrangment.

In the FEM model, the nonlinear characteristics of each layer have been taken into consideration separately, and the simulation has been carried out for all samples, including baseline bonded and hybrid magnets and parallel and series arrangements.

It should be highlighted that an electrical circuit has been coupled with the electromagnetic model to control and measure the demagnetization current.

Fig. 20 compares the flux density in the middle of the defined air gap for the single-layer magnets made of the baseline materials, computed by 3D-FEM with the experimental measurements. The FEM results are in good agreement with the experience. Once again, it was observed that the calculated and measured induction in the air gap for hybrid 70 % magnet is not well matched. The reason would be due to the measurement error and the accuracy of the instrument used for the measurement. However, it should be highlighted that measuring the flux density in the range of 0.1 T is quite challenging and tricky, especially in magnetic circuits with very small air gaps.

The same simulation model has been applied for the multilayer magnet, and 3D-FEM has computed the flux density in the middle of the air gap. Fig. 20 and Fig. 21 represent the comparison of the FEM and experimental results for samples having series and parallel arrangements, respectively. The simulation results are approximately matched with those of the experiment. However, Fig. 22 shows that there are still some differences, particularly for the parallel 70 % sample at values lower than 0.15 T, which are due to the instrumentation's limitation at low flux density/demagnetization currents. Moreover, the hysteresisgraph sensor coil needs to be perfectly uniform with respect to the cross-section of the magnets; with actual arrangements, it is not possible to ensure the correct position of the sensing coil.

In addition, in the first approximation, the predicted values are promising; however, further optimization will be done to achieve better matching between measurement and simulation in the future. Finally, it should be noted that the material used in the structure of the electromagnetic circuit was unknown, and typical magnetic construction steel has been considered in the simulations. Thus, the difference in air gap flux density when no current flows into the circuit is probably due to the different permeability of the pure iron and real material used in the structure of the hysteresisgraph.

Both the measured and simulated results allow extracting useful information on the behaviour of the presented materials. The presence of an air gap in the magnetic circuit gives immediate feedback of the air gap induction against magnet type, geometry and external field, making possible quick parallelism to the magnetic structure of a rotating electrical machine. The good agreement between simulations and measurements reasonably allows applying the simulations to a wide range of new material and airgap configurations.

VII. Conclusion

This study investigates two types of hard magnetic materials with different magnetic and mechanical properties to obtain a unified double-layer magnet block for electrical machine application.

Some samples of multilayer magnets have been prepared by means of bonded and hybrid magnetic composite powdered materials, proving the feasibility of the proposed technology. The samples have been characterized using a particular magnetic circuit based on a conventional hysteresisgraph. The same setup was provided with a small air gap, making it suitable to equivalently investigate the air gap magnetic behavior of rotating electrical machines. In addition, the series and parallel multilayer arrangements have been designed and studied. It has been found that the double-layer magnets with parallel arrangement can be demagnetized easier than series arrangement. Besides, the series configurations are stronger in terms of energetic behavior, meaning the maximum remanence and BH_{max}. Due to the experimental validation, the self-produced double-layer magnets could be considered as potential candidates suitable for variable flux permanent magnet synchronous machines. Additionally, a complete model has been implemented through 3D-FEM of the proposed magnetic circuit used during the characterization. This model provides proof of the concept for future simulation-based studies, reducing the time to obtain a functional prototype.

VIII. References

[1] F. Fiorillo, "Magnetic materials for electrical applications: A Review," Torino, 2010. doi: 10.13140/RG.2.2.21142.14407.

[2] J. F. Gieras, *Permanent magnet motor technology: design and applications*. CRC press, 2009.

[3] J. M. D. Coey, "Permanent magnet applications," *J. Magn. Magn. Mater.*, vol. 248, no. 3, pp. 441–456, 2002.

[4] H. Tahanian, M. Aliahmadi, and J. Faiz, "Ferrite permanent magnets in electrical machines: opportunities and challenges of a non-rare-earth alternative," *IEEE Trans. Magn.*, vol. 56, no. 3, pp. 1–20, 2020.

[5] H. Nakamura, "The current and future status of rare earth permanent magnets," *Scr. Mater.*, vol. 154, pp. 273–276, 2018.

[6] B. E. Davies, R. S. Mottram, and I. R. Harris, "Recent developments in the sintering of NdFeB," *Mater. Chem. Phys.*, vol. 67, no. 1–3, pp. 272–281, 2001.

[7] Steve Constantinides, "Manufacture of Modern Permanent Magnet Materials." Arnold Magnetic Technologies Corp., Rochester, NY, USA, pp. 1–12, 2014.

[8] E. Poskovic, L. Ferraris, F. Carosio, F. Franchini, and N. Bianchi, "Overview on bonded magnets realization, characterization and adoption in prototypes," in *IECON 2019-45th Annual Conference of the IEEE Industrial Electronics Society*, 2019, vol. 1, pp. 1249–1254.

[9] L. Ferraris, F. Franchini, and E. Pošković, "Hybrid magnetic composite (HMC) materials for sensor applications," in *2016 IEEE Sensors Applications Symposium (SAS)*, 2016, pp. 1–6.

[10] L. Ferraris, E. Poskovic, and F. Franchini, "Study of the compositions of hybrid magnetic composite (HMC) materials for sensor applications," in *2018 20th European Conference on Power Electronics and Applications (EPE'18 ECCE Europe)*, 2018, p. P-1.

[11] M. A. Darmani, E. Poskovic, L. Ferraris, and A. Cavagnino, "Multiple Layer Compression of SMC and PM Powdered Materials," in *IECON 2019 - 45th Annual Conference of the IEEE Industrial Electronics Society*, Oct. 2019, pp. 1216–1221, doi: 10.1109/IECON.2019.8927574.

[12] V. Ostovic, "Memory motors," *IEEE Ind. Appl. Mag.*, vol. 9, no. 1, pp. 52–61, 2003.

[13] K. Sakai, K. Yuki, Y. Hashiba, N. Takahashi, and K. Yasui, "Principle of the variable-magnetic-force memory motor," in *2009 International Conference on Electrical Machines and Systems*, 2009, pp. 1–6.

[14] H. Yang, H. Zheng, Z. Q. Zhu, H. Lin, S. Lyu, and Z. Pan, "Comparative study of partitioned stator memory machines with series and parallel hybrid PM configurations," *IEEE Trans. Magn.*, vol. 55, no. 7, pp. 1–8, 2019.

[15] R. Imamura, T. Wu, and R. D. Lorenz, "Design of variable magnetization pattern machines for dynamic changes in the back EMF waveform," *IEEE Trans. Ind. Appl.*, vol. 55, no. 4, pp. 3469–3478, 2019.

[16] A. Athavale, K. Sasaki, B. S. Gagas, T. Kato, and R. D. Lorenz, "Variable flux permanent magnet synchronous machine (VF-PMSM) design methodologies to meet electric vehicle traction requirements with reduced losses," *IEEE Trans. Ind. Appl.*, vol. 53, no. 5, pp. 4318–4326, 2017.

[17] G. Qiao, M. Wang, F. Liu, Y. Liu, and P. Zheng, "Analysis of Novel Hybrid-PM Variable-Flux PMSMs With Series–Parallel Magnetic Circuits," *IEEE Trans. Magn.*, vol. 57, no. 2, pp. 1–6, 2020.

[18] M. A. Darmani, E. Poskovic, F. Franchini, L. Ferraris, and A. Cavagnino, "Multiple Layer Magnetic Materials for Variable Flux Permanent Magnet Machines," in *2020 International Conference on Electrical Machines (ICEM)*, Aug. 2020, vol. 1, pp. 1662–1668.

[19] M. A. Darmani, E. Poskovic, S. Vaschetto, F. Franchini, L. Ferraris, and A. Cavagnino, "Multilayer Bonded Magnets in Surface-Mounted PM Synchronous Machines," in *2020 IEEE Energy Conversion Congress and Exposition (ECCE)*, Oct. 2020, pp. 1052–1059.

[20] F. Fiorillo, *Measurement and characterization of magnetic materials (electromagnetism)*. Elsevier Academic Press, 2005.

[21] B. Barman and A. Petrou, "Measuring the magnetization of a permanent magnet," *Am. J. Phys.*, vol. 87, no. 4, pp. 275–278, 2019.

[22] G. C. Hadjipanayis, *Bonded Magnets: Proceedings of the NATO Advanced Research Workshop on Science and Technology of Bonded Magnets Newark, USA 22–25 August 2002*, vol. 118. Springer Science & Business Media, 2012.

[23] C. Chien, *The Hall effect and its applications*. Springer Science & Business Media, 2013.

[24] S. Foner, "Vibrating sample magnetometer," *Rev. Sci. Instrum.*, vol. 27, no. 7, p. 548, 1956.

[25] F. Fiorillo, "Measurements of magnetic materials," *Metrologia*, vol. 47, no. 2, p. S114, 2010.

[26] S. Möwius, N. Kropff, and M. Velicescu, "Measurement technologies for permanent magnets," *ACTA IMEKO*, vol. 7, no. 4, 2018.

[27] R. Allcock and S. Constantinides, "Magnetic Measuring Techniques for Both Magnets and Assemblies," *Arnold Magn. Technol. Rochester, NY, USA*, 2012.

[28] I.-I. E. Commission, "Magnetic materials - Part 5: Permanent magnet (magnetically hard) materials - Methods of measurement of magnetic properties, IEC 60404-5." 2015.

Mostafa Ahmadi Darmani (S'19–M'22) was born in Tehran, Iran, in 1987. He received his M.Sc. degree in electrical engineering in 2013 from Azad University in Tehran, Iran. From 2013 to 2018, He worked in Iran as an electrical engineer and consultant in different industries and instructor in training centres. He is currently working towards his PhD degree in electrical engineering with the Department of Energy at Politecnico di Torino, Italy. His main research interests include multi-physics design and modelling of electrical machines. He is a Member of IEEE Industry Application Society, Industrial Electronics Society, and IEEE IAS Electric Machines Committee. He serves as a reviewer for several IEEE Transactions and international journals and conferences.

Emir Pošković was born in Sarajevo in Bosnia and Herzegovina, He studied and graduated from the Polytechnic of Turin, where he received B.S. and M.Sc. degree in electrical engineering in 2006 and in 2008, respectively. Also, he received a doctor's degree in electrical energy engineering from the University of Padova

in 2020. He is an Assistant Professor with the Energy Department, Politecnico di Torino and a Key Researcher for the Magnetic Characterization Laboratory, Alessandria campus of Politecnico di Torino. His special fields of interest included soft and hard magnetic materials, electrical machines, alternative and renewable energy (micro-hydro, fuel cell, PV-photovoltaic). He has published more than 50 scientific papers in conference proceedings and technical journals.

Fausto Franchini received the B.S. degree in electrical engineering from the Politecnico di Torino, Alessandria, Italy, in 2003. Since 2004, he has been a Technician with the Electrical Engineering Laboratory, Politecnico di Torino, where he has been responsible of the laboratory since 2007. His fields of interest include electromagnetic metrology, electromagnetic compatibility, data acquisition, control, and automation.

Luca Ferraris received the M.S. degree in electrical engineering from the Politecnico di Torino, Turin, Italy, in 1992. In 1995, he joined the Department of Electrical Engineering, Politecnico di Torino, where he is currently an Associate Professor of Electrical Machines and Drives and currently coordinates the experimental activities of the Electric and Electromagnetic Laboratories. He has published more than 110 technical papers in conference proceedings and technical journals. His research interests are the energetic behavior of machines, innovative magnetic materials for electromagnetic devices, electrical traction, electromagnetic compatibility, and renewable energies.

Andrea Cavagnino (M'04–SM'10–F'20) was born in Asti, Italy, in 1970. He received his M.Sc. and Ph.D. degrees in electrical engineering from the Politecnico di Torino, Italy, in 1995 and 2000, respectively. He is a professor at the Politecnico di Torino. He has authored or co-authored more than 250 papers, receiving four Best Paper Awards. His research interests include electromagnetic design, thermal design, and energetic behaviour of electrical machines. He usually cooperates with factories for a direct technological transfer and he has been involved in several public and private research projects. Prof. Cavagnino is an Associate Editor of the IEEE TRANSACTIONS ON ENERGY CONVERSION (TEC), a Past Chair of the Electrical Machines Technical Committee of the IEEE Industrial Electronics Society, a past Associate Editor of the IEEE TRANSACTIONS ON INDUSTRIAL ELECTRONICS (TIE), and the IEEE TRANSACTIONS ON INDUSTRY APPLICATIONS. He was also a Guest Editor of six Special Sections for IEEE-TIE and co-Editor in Chief of a Special Issue for IEEE-TEC. Prof. Cavagnino was a technical program chair of the IEEE-IEMDC 2015 and IEEE-ECCE 2022 conferences. He is a reviewer for several IEEE TRANSACTIONS and other international journals and conferences.